JOC The Journal of Organic Chemistry

pubs.acs.org/joc Note

A Biotinylated Glycosylphosphatidylinositol (GPI) as the Universal Platform To Access GPI-Anchored Protein Analogues

Xin Yan,[§] Jiatong Guo,[§] Sayan Kundu, and Zhongwu Guo*

Cite This: J. Org. Chem. 2024, 89, 1345−1352 Read Online

ACCESS | Metrics & More | Article Recommendations | Supporting Information

ABSTRACT: A glycosylphosphatidylinositol (GPI) derivative with biotin linked to its mannose III 6-O-position was prepared by a convergent strategy. This biotinylated GPI was demonstrated to bind avidinated proteins readily through biotin−avidin interaction and, therefore, can serve as a universal platform to access various biologically significant GPI-anchored protein analogues.

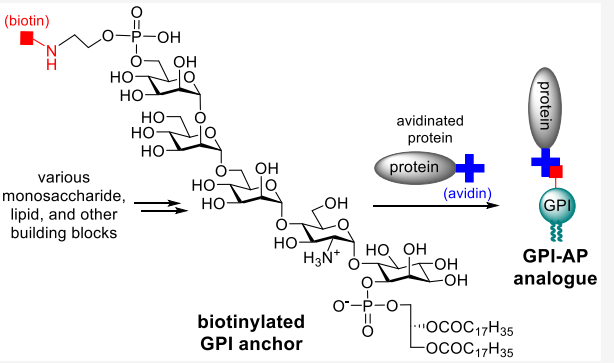

Glycosylphosphatidylinositols (GPIs) are a class of unique and ubiquitous glycolipids in eukaryotes. They are typically attached to the C-terminus of proteins, which represents one of the most common and important posttranslational modifications.[1−3] GPI-linked proteins are anchored onto the cell surface via embedding their lipid tails in the outer leaflet of the membrane bilayer. To date, several hundred GPI-anchored proteins (GPI-APs), including at least 150 from humans, have been identified[4,5] and demonstrated to play a critical role in various physiological and pathological processes.[6−8] For example, GPI-APs are important receptors on the cell surface to regulate many cellular activities from recognition to signal transduction.[9−11] It has been further disclosed that GPI-APs would not function properly without GPI anchors or having GPIs replaced by other anchoring mechanisms.[12−16] To investigate GPI-APs and understand their functions, it is necessary to have appropriate GPI-AP probes.

However, it is difficult to access GPI-APs. Isolating GPI-APs from cells is impractical due to their low natural abundance and their heterogeneous structure and amphiphilic property.[17] There is not a practical method for the synthesis of GPI-APs and their analogues either, although several approaches have been explored to tackle this problem. As illustrated in Figure 1A, most GPI-APs have proteins attached to the phosphorylethanolamine (PE) moiety at the 6-O-position of mannose III (Man-III) in the conserved core structure of GPI anchors. Thus, all the reported methods for GPI-AP synthesis are based upon a similar strategy, i.e., preparing the proper GPI and protein derivatives separately and finally stitching them together by a chemo-/regioselective reaction. Native chemical ligation (NCL) was used by Bertozzi,[18] Seeberger,[19] and Varón Silva[20] groups to couple cysteine (Cys)-modified GPIs or GPI mimics with C-terminal thioesters of proteins to afford GPI-AP analogues with a Cys residue between the GPI and protein (Figure 1B). Our group used a bacterial sortase to attach glycine (Gly)-modified GPIs to proteins having a sorting signal at the C-terminus to prepare GPI-AP analogues that have a short peptide between the GPI and protein (Figure 1B).[21−23] A significant drawback of these synthetic methodologies is that they are difficult to achieve or have limited scopes. For instance, protein thioesters and Cys-modified GPIs required for NCL are not easily available, while the sortase-based method is not readily applicable to fully lipidated GPIs because of their poor solubility in aqueous solution where enzymatic reactions are carried out. Our group has also investigated total synthesis.[24−26] Although this approach could afford GPI-anchored peptides/glycopeptides, its application to full-size proteins is limited, as it is impractical to obtain protected proteins for regioselective coupling with GPIs. In addition, the Mootz group combined genetic engineering with bioconjugation to generate GPI-APs on cells,[27] but this method has not been employed to prepare homogeneous GPI-APs. Clearly, innovative methods to access GPI-APs and GPI-AP analogues are highly desired.

Received: November 7, 2023
Revised: December 6, 2023
Accepted: December 8, 2023
Published: December 28, 2023

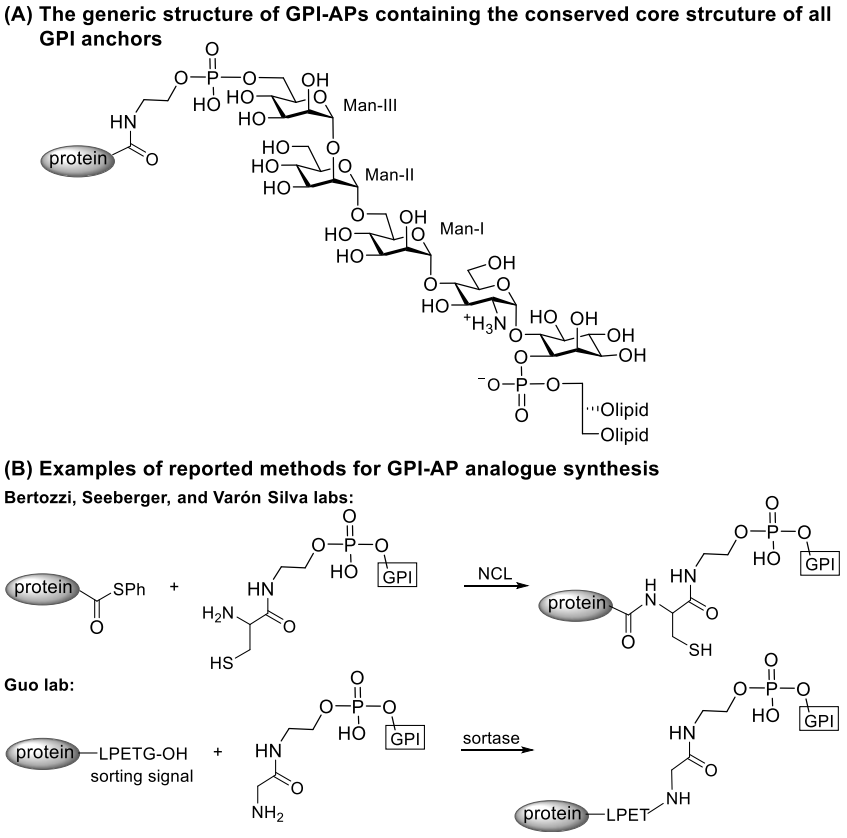

Figure 1. Generic structure of GPI-APs containing the conserved core structure of natural GPI anchors (A) and representative methods explored for the synthesis of GPI-AP analogues (B).

The aim of this research is to develop a new and practical preparation method for GPI-AP analogues. Particularly, we are interested in a versatile and universal platform that can be utilized to access various GPI-APs by a reliable and streamlined protocol. To this end, the biotin−avidin conjugation system is especially attractive due to its convenience, efficiency, and flexibility.[28,29] For example, the noncovalent binding between biotin and avidin is easily achievable under physiological conditions. In the meantime, biotin−avidin binding is extremely strong, similar to some covalent bonds.[30,31] As a result, the biotin−avidin conjugation system finds broad applications in biological research.

Accordingly, we have designed GPI derivative **1** (Figure 2), which has biotin linked to the conserved PE moiety at the Man-III 6-O-position of GPIs, as a universal substrate for GPI-AP analogue preparation. As illustrated in Figure 2, any avidinated protein can be conjugated with biotinylated **1** to generate GPI-AP analogue **2** based on the strong interactions between biotin and avidin or streptavidin. In turn, avidinated proteins can be readily prepared by fusion protein technologies, while many avidinated proteins are commercially available as well. Here, we report the synthesis of **1** and its application to preparing GPI-AP analogues and other GPI conjugates.

The synthesis of **1** started with the preparation of **12** (Scheme 1) by a method similar to that developed by our group for other GPI derivatives,[32] utilizing pseudopentasaccharide **11** as the key intermediate. In turn, **11** was assembled by a convergent [3 + 2] glycosylation strategy. After trimannosyl imidate **9** as the glycosyl donor and lipidated pseudodisaccharide **10** as the glycosyl acceptor were prepared

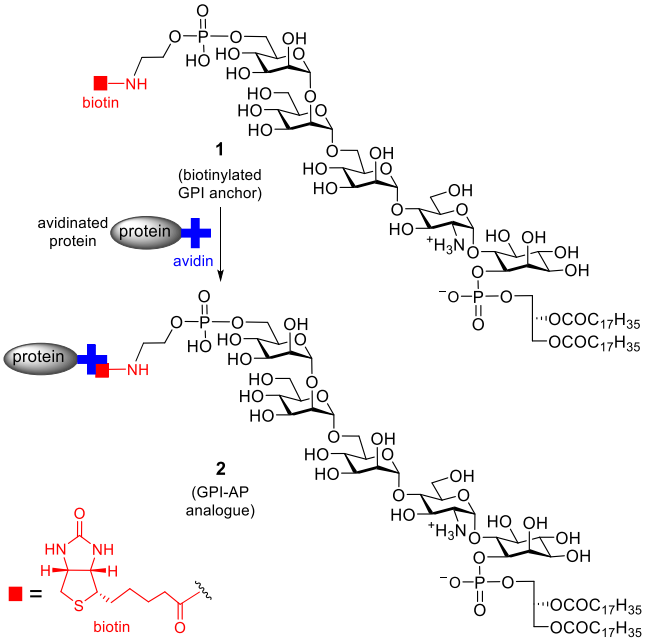

Figure 2. Design of a biotinylated GPI anchor **1** as a universal platform for accessing GPI-AP analogues **2** via the strong affinity between biotin in **1** and avidin/streptavidin in fusion proteins.

from monosaccharide and lipid building blocks **3**−**8** according to reported procedures,[32−37] **10** was glycosylated with **9** in the presence of trimethylsilyl triflate (TMSOTf) to provide **11** as a mixture of epimers (due to the stereogenic phosphorus center) in a good yield. Selective removal of the *tert*-butyldimethylsilyl

https://doi.org/10.1021/acs.joc.3c02560
J. Org. Chem. 2024, 89, 1345−1352

Scheme 1. Synthesis of Key Intermediate 12

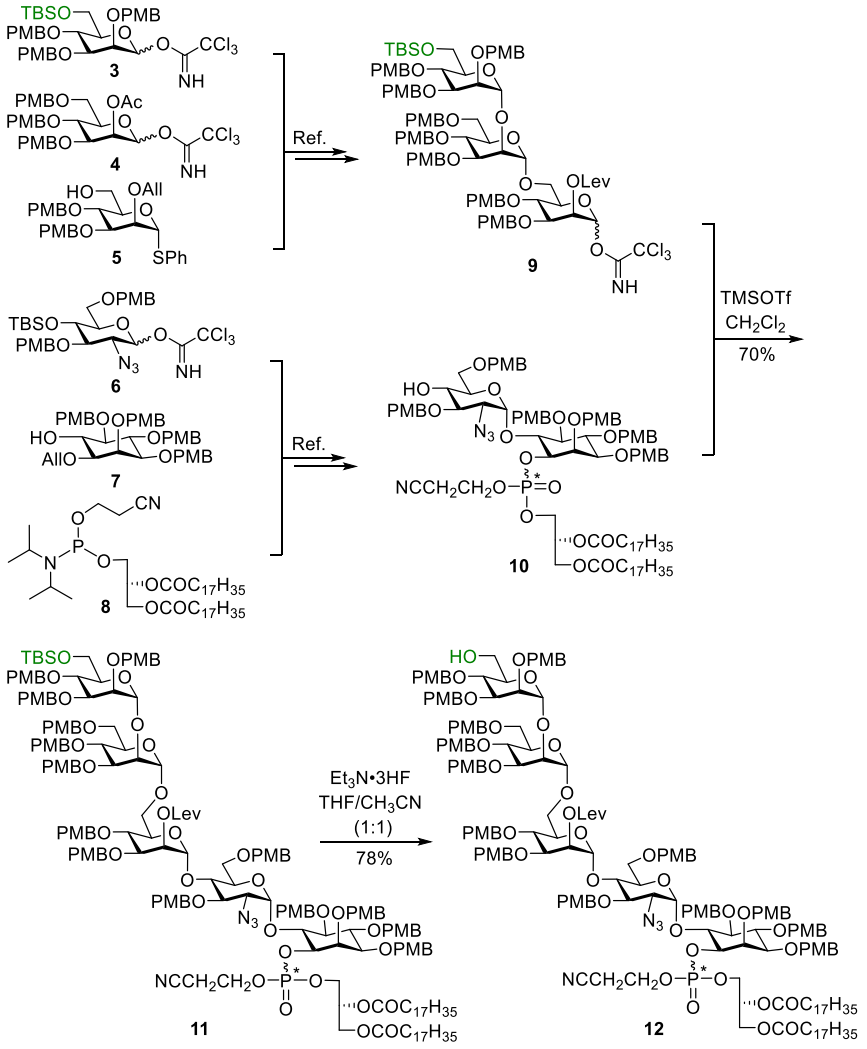

(TBS) group at the Man-III 6-O-position utilizing 3HF·Et_3N gave alcohol **12**[32] that was ready for the introduction of biotinylated PE.

To assemble the synthetic target **1** (Scheme 2), we first linked biotin to ethanolamine to obtain **13** and then converted **13** into biotinylated phosphoramidite **14** via reacting with 2-cyanoethyl *N*,*N*,*N*′,*N*′-tetraisopropylphosphorodiamidite in the presence of diisopropylammonium tetrazolide by a reported procedure.[38] Next, highly reactive **14** was employed without further purification for the phosphorylation of **12** by a one-pot−two-step approach,[39,40] including coupling **12** with **14** in dichloromethane (DCM)/CH_3CN (9:1) promoted by tetrazole and then oxidation of the product with I_2, to give **15** (76%). Finally, **15** was deprotected in three steps, including removal of the *O*-levulinoyl (Lev) group using hydrazine acetate, reduction of the azide with simultaneous removal of the cyanoethyl group using 1,3-propanedithiol and diisopropylethylamine (DIPEA) in aqueous pyridine, and removal of all PMB groups with 10% TFA (trifluoroacetic acid) in DCM, to provide biotinylated GPI anchor **1** (78%, three steps). The progress of each reaction was monitored with MS, and **1** was finally purified by size exclusion chromatography using a Sephadex LH-20 column and characterized with NMR and high-resolution (HR) MS data. The HR MS results further revealed that a part of the product was oxidized in the deprotection process (mainly during TFA treatment), while this side product was inseparable from **1**. We anticipated that the oxidation reaction occurred to biotin, since it was not observed in our previous syntheses of GPIs that did not contain biotin. In addition, biotin was shown to be easily oxidized during chemical synthesis or in the freeze/thaw process.[41,42] Nonetheless, this oxidation does not cause concern for the biological application of the product because biotin sulfoxide can also bind to avidin strongly and has been widely used in biological studies.[43,44]

To verify that biotinylated GPI **1** can serve as a general platform to prepare biologically useful GPI-AP analogues, we studied its capacity to bind avidinated biomolecules for their anchorage to the cell membrane, utilizing liposomal mimics and sandwich enzyme-linked immunosorbent assay (ELISA). Hence, we prepared liposomes (∼100 nm) of **1** (1 mol %) using 1-palmitoyl-2-oleoyl-*sn*-glycero-3-phosphocholine (POPC) by the conventional extrusion method[45] and employed them to coat streptavidin-modified ELISA plates (Figure 3A). First, we used the liposome-coated ELISA plate to validate the biotinylation of liposomes and their binding to avidinated proteins. Since each liposome contains multiple copies of biotinylated GPIs, it can bind streptavidin-modified ELISA plate and molecules, such as avidin−protein conjugates, concurrently (Figure 3A). In this context, we incubated the

https://doi.org/10.1021/acs.joc.3c02560
J. Org. Chem. 2024, 89, 1345−1352

Scheme 2. Assembly of the Synthetic Target 1

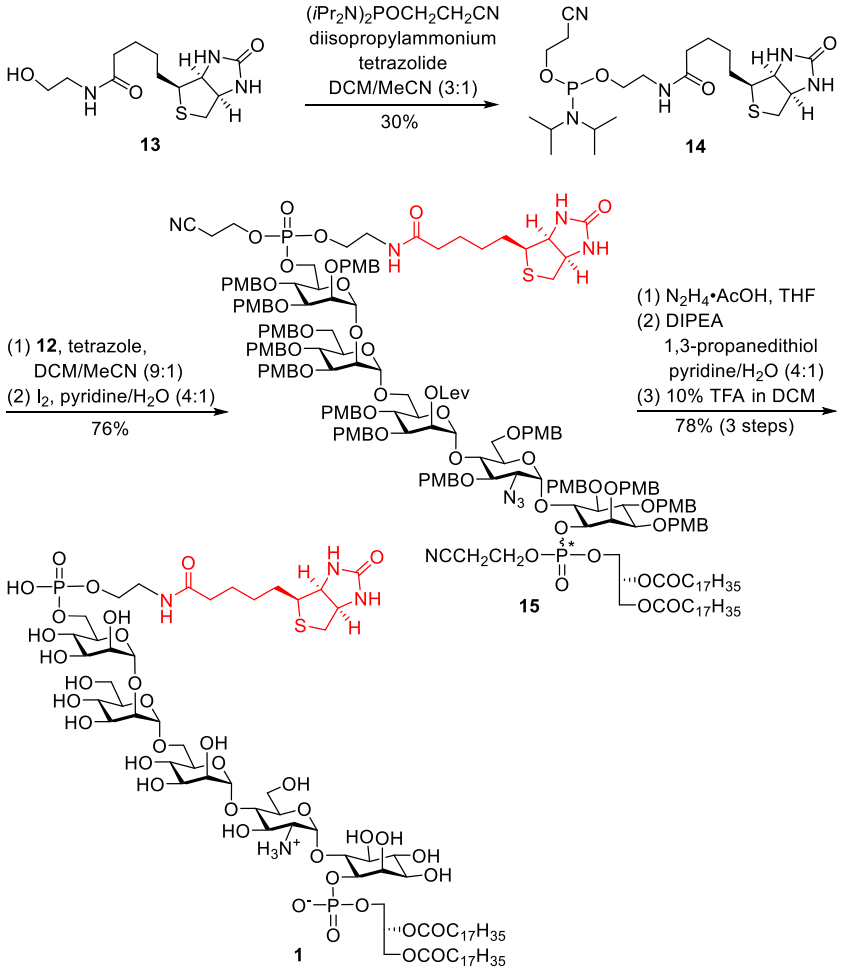

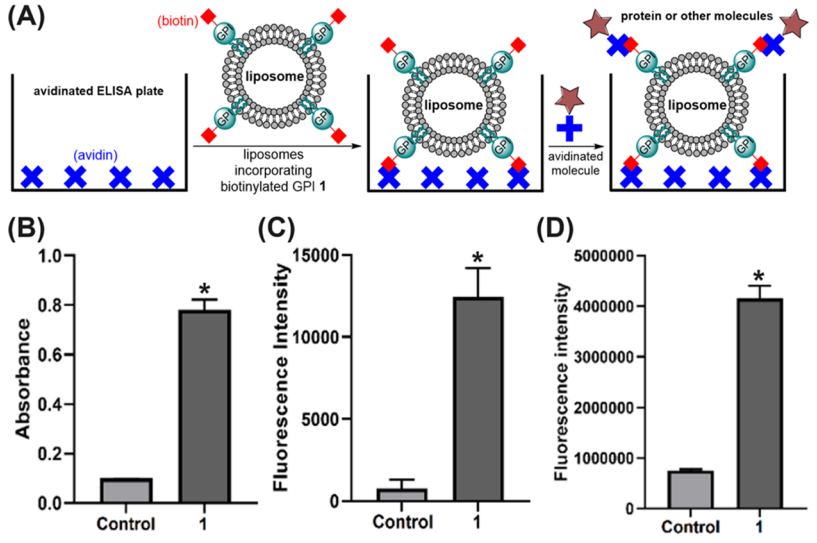

Figure 3. (A) The experimental protocol to attach **1**-functionalized liposomes to ELISA plates and then avidinated molecules to the liposomes via biotin−avidin interaction. (B) Light absorbances (at 405 nm) of the plates coated with **1**-functionalized liposomes or with liposomes without **1** (control) after sequential treatments with streptavidin−ALP and PNPP. (C) Fluorescence intensities of ELISA plates coated with **1**-functionalized or control liposomes after streptavidin−A488 treatment. (D) Fluorescence intensities of the PBS suspensions of **1**-functionalized and control liposomes treated with streptavidin-A488. The results are expressed as average ± standard deviation of triplicate experiments. *$P < 0.01$: Difference is statistically significant compared to the control.

liposome-coated plates with streptavidin−alkaline phosphatase (ALP) conjugate and examined ALP attachment to liposomes by analyzing its reaction with *p*-nitrophenyl phosphate (PNPP). ALP can hydrolyze PNPP to release *p*-nitrophenol

https://doi.org/10.1021/acs.joc.3c02560
J. Org. Chem. 2024, 89, 1345−1352

that is quantifiable via measuring the absorbance of light at 405 nm wavelength using a plate reader, thereby revealing the quantities of ALP attached to liposomes on the plate. Our results (Figure 3B and Table S1 of SI) revealed that, compared to liposomes without **1** (the negative control), **1**-functionalized liposomes showed a significant increase in light absorbance (by about 8-fold). Next, we investigated the binding of avidinated fluorophores to the liposomes on plates, also by sandwich ELISA. It was shown that incubating the liposome-coated plates with streptavidinated A488, which is a green fluorophore, resulted in a significant increase in the fluorescence intensity of liposomes functionalized with **1**, as compared to the negative control (Figure 3C and Table S2 of SI). These results have validated the successful biotinylation of liposomes with **1** and attachment of **1**-functionalized liposomes to avidin-modified ELISA plates, as well as the efficient attachment of both proteins and small molecule fluorescent tags to **1** and **1**-functionalized liposomes on the plate.

We also examined the attachment of avidinated molecules to **1**-functionalized liposomes in solution. In this experiment, we directly treated the liposomes suspended in 4-(2-hydroxyethyl)-1-piperazineethanesulfonic acid (HEPES) buffer with streptavidin-A488. After centrifugal filtration using a filter of 100 kDa pore size and washing to remove nonmembrane-bound streptavidin−A488 that has a MW of 60 kDa, the resultant liposomes were subjected to fluorescence study. Liposomes functionalized with **1** showed significantly higher fluorescence intensity than liposomes of the control group (Figure 3D and Table S3 of SI). Moreover, fluorescence microscopic analysis of the samples also revealed strong green fluorescence of **1**-functionalized liposomes (Figure S1 of SI). These results have provided another piece of evidence that supports the efficient attachment of avidinated/streptavidinated molecules to **1** and **1**-containing liposomes.

In summary, a new, biotinylated GPI derivative **1** was synthesized by a convergent strategy, which is highlighted by the assembly of its core glycan via [3 + 2] glycosylation. Streptavidin−A488 and streptavidin−ALP conjugates were conveniently and efficiently attached to **1** and its liposomes via avidin−biotin interaction. It is anticipated that other avidinated/streptavidinated proteins and molecules can also be readily coupled with this biotinylated GPI analogue. Therefore, **1** may serve as a new, universal platform to access various GPI-AP analogues and other biologically significant GPI conjugates, underscoring the promise of **1** for the investigation of GPIs and GPI-APs.

EXPERIMENTAL SECTION

Synthesis of 6-*O*-{[6-*O*-(*tert*-Butyldimethylsilyl)-2,3,4-tri-*O*-(*p*-methoxybenzyl)-α-D-mannopyranosyl]-(1→2)-[3,4,6-tri-*O*-(*p*-methoxybenzyl)-α-D-mannopyranosyl]-(1→6)-[3,4-di-*O*-(*p*-methoxybenzyl)-2-*O*-(4-oxopentanoyl)-α-D-mannopyranosyl]-(1→4)-[2-azido-2-deoxy-3,6-di-*O*-(*p*-methoxybenzyl)-α-D-glucopyranosyl]}-1-*O*-[(2-cyanoethoxyl)-(1,2-di-*O*-stearoyl-*sn*-glycerol)-phosphono]-2,3,4,5-tetra-*O*-(*p*-methoxybenzyl)-*myo*-inositol (11). Compounds **9** (53.0 mg, 29.2 μmol) and **10** (25.0 mg, 13.7 μmol), which were prepared according to reported methods and gave the same NMR spectra (SI) as those in the literature,[32] dissolved in dry DCM/Et_2O (4:1, 2.0 mL) were mixed with MS 4 Å (10.0 mg), and the suspension was stirred under an N_2 atmosphere at rt for 30 min. After being cooled to 0 °C, TMSOTf (1.1 μL, 6.00 μmol) was added to the mixture. After the mixture was stirred for another 20 min and **9** was consumed as indicated by TLC, the reaction mixture was diluted with DCM, poured into saturated aq $NaHCO_3$ solution, and filtered through a Celite pad. After extraction and separation of the aq layer with DCM (3 × 10 mL), the combined organic phase was dried over Na_2SO_4 and concentrated in vacuum. The crude product was then purified by flash silica column chromatography (hexane/EtOAc = 1:1) to provide **11** (33.5 mg, 9.51 μmol, 70%). R_f = 0.5 (hexane/EtOAc = 1:1). The anomeric configurations of this pentasaccharide were confirmed by GD ^{13}C and $^1H-^{13}C$ coupled HSQC NMR data. ^1H NMR (600 MHz, $CDCl_3$): δ 7.32−7.02 (m, 28H), 6.88−6.78 (m, 28H), 5.43 (m, 1H, Man-I-2), 5.37 (d, J = 3.7 Hz, 1H, $GlcN_3$-1), 5.34 (s, 1H, Man-1), 5.27 (m, 0.5H, Gly-2), 5.22 (m, 1.5H, Gly-2 and Man-1), 4.83 (s, 1H, Man-1), 3.81 (s, 3H), 3.79 (s, 3H), 3.74−3.72 (s, multiple), 3.63 (s, 3H), 3.62 (s, 3H), 3.60 (s, 3H), 3.42 (s, 3H), 3.39 (m, 1H), 3.32−3.23 (m, 2H), 3.17 (m, 1H), 2.77 (m, 1H), 2.63 (m, 1H), 2.30 (m, 4H), 2.08 (m, 1H), 2.05 (s, 3H), 1.58 (m, 8H), 1.33−1.22 (m, 56H), 0.88 (t, J = 6.9 Hz, 6H), 0.86 (s, 9H), 0.04 (s, 3H), 0.03 (s, 3H). $^{13}C\{^1H\}$ NMR (151 MHz, $CDCl_3$): δ 205.9, 193.4, 177.2, 173.3 (2 C), 173.0, 172.9, 171.9, 159.3, 159.2, 159.1 (2 C), 159.0 (2 C), 157.8, 131.5, 131.2, 131.1, 131.0 (2C), 130.9, 130.8, 130.4, 130.3 (2 C), 130.1 (2C), 129.9, 129.7, 129.6 (2 C), 129.4 (4 C), 129.2, 129.1 (2C), 116.5, 116.0, 113.9−113.6 (multiple C), 113.2, 110.5, 107.0, 99.5 (Man-1), 99.3 (Man-1), 98.8 (Man-1), 97.8 ($GlcN_3$-1, diastereomers), 81.4, 81.1, 80.6, 80.5, 80.3, 79.9, 79.6, 78.3, 76.5, 76.3, 75.5, 75.2, 75.0, 74.9, 74.7, 74.6, 74.4, 73.7, 73.6, 73.3, 73.0, 72.8, 72.7, 72.2, 71.8, 71.7, 71.4, 71.3, 70.1, 69.9, 69.5, 69.2, 68.9, 68.3, 67.1, 66.5, 66.3, 64.3, 63.2, 62.8, 62.6, 62.4, 62.0, 61.6, 58.3, 55.4, 55.3, 55.3, 55.3, 55.2, 55.2, 55.1, 51.0, 38.0, 36.5, 34.3, 34.2, 34.1, 34.1, 33.8, 33.4, 32.1, 31.6, 30.3, 29.8−29.7 (multiple C), 29.5 (3 C), 29.3, 29.2, 28.2, 26.9, 26.8, 26.1, 25.7, 25.5, 25.0, 24.9, 23.3, 22.8, 22.1, 19.7, 19.0, 18.5, 17.9, 17.6, 16.9, 14.3, 13.2, −4.8, −5.1, −7.6. GD ^{13}C NMR (151 MHz, $CDCl_3$, ^1H-coupled) and ^{13}C signals derived from $^1H-^{13}C$ coupled HSQC NMR (600/151 MHz, $CDCl_3$): δ 99.5 (d, $^1J_{C\text{-}1,H\text{-}1}$ = 170.1 Hz), 99.3 (d, $^1J_{C\text{-}1,H\text{-}1}$ = 172.9 Hz), 98.8 (d, $^1J_{C\text{-}1,H\text{-}1}$ = 168.1 Hz), 97.8 (d, $^1J_{C\text{-}1,H\text{-}1}$ = 173.1 Hz, $GlcN_3$-1). $^{31}P\{^1H\}$ NMR (243 MHz, $CDCl_3$): δ −2.4, −2.9. HR ESI-TOF-MS m/z: calcd for $C_{195}H_{269}N_6O_{48}PSi$ $[M + 2NH_4]^{2+}$, 1760.9144; found, 1760.9194.

Synthesis of 6-*O*-{[2,3,4-Tri-*O*-(*p*-methoxybenzyl)-α-D-mannopyranosyl]-(1→2)-[3,4,6-tri-*O*-(*p*-methoxybenzyl)-α-D-mannopyranosyl]-(1→6)-[3,4-di-*O*-(*p*-methoxybenzyl)-2-*O*-(4-oxopentanoyl)-α-D-mannopyranosyl]-(1→4)-[2-azido-2-deoxy-3,6-di-*O*-(*p*-methoxybenzyl)-α-D-glucopyranosyl]}-1-*O*-[(2-cyanoethoxyl)-(1,2-di-*O*-stearoyl-*sn*-glycerol)-phosphono]-2,3,4,5-tetra-*O*-(*p*-methoxybenzyl)-*myo*-inositol (12). Compound **11** (12.0 mg, 3.44 μmol, 1.0 equiv) was added to anhydrous THF/CH_3CN (1:1, 2.0 mL) at rt, which was followed by 3HF·Et_3N (0.3 mL). After being stirred overnight, the reaction was quenched by dropwise addition of saturated aq $NaHCO_3$. The aqueous layer was extracted with EtOAc (3 × 10 mL), and the combined organic layer was dried over Na_2SO_4 and concentrated in vacuum, and the product was purified by flash silica gel column chromatography to give **12** (9.00 mg, 2.67 μmol, 78%) as colorless syrup. R_f = 0.40 (hexane/EtOAc = 1:1). ^1H NMR (600 MHz, $CDCl_3$, partial): δ 7.32−7.07 (m, 28 H), 6.88−6.78 (m, 28 H), 5.45 (m, 1 H, Man-I-2), 5.38 (d, J = 3.7 Hz, 1 H, $GlcN_3$-1), 5.35 (s, 1 H, Man-1), 5.27 (m, 0.5 H, Gly-2), 5.22 (m, 0.5 H, Gly-2), 5.09 (s, 1 H, Man-1), 4.84 (s, 1 H, Man-1), 3.81 (s, 3 H), 3.78 (s, 3 H), 3.74−3.72 (s, multiple), 3.64 (s, 3 H), 3.62 (s, 3 H), 3.60 (s, 3 H), 3.42 (s, 3 H), 3.39 (td, J = 9.3, 3.3 Hz, 1 H), 3.32−3.23 (m, 2 H), 3.17 (ddd, J = 10.8, 8.5, 3.7 Hz, 1 H), 2.77 (dq, J = 11.1, 5.7, 5.0 Hz, 1 H), 2.63 (dt, J = 14.7, 6.3 Hz, 1 H), 2.30 (dq, J = 22.1, 7.6 Hz, 4 H), 2.08 (dd, J = 8.9, 3.7 Hz, 1 H), 2.05 (s, 3 H), 1.58 (dd, J = 8.1, 4.2 Hz, 8 H), 1.33−1.22 (m, 56 H), 0.88 (t, J = 6.9 Hz, 6 H). $^{13}C\{^1H\}$ NMR (151 MHz, $CDCl_3$, derived from HSQC spectrum): δ 129.6−129.0 (multiple C), 113.8−113.7 (multiple C), 99.6 (Man-1), 99.3 (Man-1), 99.2 (Man-1), 97.7 ($GlcN_3$-1, diastereomers), 81.3, 80.4 (3 C), 80.3, 79.5 (3 C), 79.4, 77.9, 77.8, 77.0, 76.5, 76.2, 75.3, 75.3, 75.1, 75.0 (2 C), 74.9, 74.9, 74.7 (5 C), 74.6 (5 C), 73.5 (2 C), 73.0 (multiple C), 72.8, 72.7, 72.5, 72.1, 71.8 (4 C), 71.5, 71.3 (2 C), 71.2, 69.9, 69.4, 69.3, 69.0, 68.9 (2 C), 68.1 (2 C), 66.2, 65.9, 65.8, 63.1, 63.0, 62.3, 62.1, 61.5 (2 C), 55.2−55.1 (multiple C), 38.0, 34.0, 32.0, 30.5, 29.8−28.8 (multiple C), 28.0 (2 C), 24.8, 22.7 (2 C), 19.7, 14.1. $^{31}P\{^1H\}$ NMR (243 MHz, $CDCl_3$): δ

https://doi.org/10.1021/acs.joc.3c02560
J. Org. Chem. 2024, 89, 1345−1352

−2.4, −2.9. HR ESI-TOF-MS m/z: calcd for $C_{189}H_{255}N_6O_{48}P$ $[M + 2NH_4]^{2+}$, 1703.8712; found, 1703.8766.

Synthesis of (*N*-Biotinyl-2-aminoethyloxy)-(2-cyanoethoxyl)-(diisopropylamino)phosphine (14). After 2-cyanoethyl *N*,*N*,*N*′,*N*′-tetraisopropylphosphorodiamidite (255 μL, 0.80 mmol, 2.0 equiv) and **13** (115 mg, 0.40 mmol, 1.0 equiv) were dissolved in anhydrous DCM/MeCN (1:1, 8.0 mL), diisopropylammonium tetrazolide (85.6 mg, 0.50 mmol, 2.0 equiv) was added to the solution. The mixture was stirred at 4 °C under N_2 overnight and then was diluted with DCM and poured into saturated aqueous $NaHCO_3$. The aqueous layer was extracted with DCM (3 × 10 mL). The organic layers were combined and dried over Na_2SO_4 and finally concentrated in vacuum. The crude material was dissolved in DCM (1 mL), and then hexane was added to precipitate **14** (58.5 mg, 0.12 mmol, 30%), which was obtained as a crude white solid product and 1:1 diastereomeric mixture originated from the phosphorus atom. ^{1}H NMR (400 MHz, $CDCl_3$): δ 6.36−6.29 (m, 1H), 5.76 (s, 1H), 5.02 (d, J = 8.0 Hz, 1H), 4.55−4.47 (m, 1H), 4.36−4.29 (m, 1H), 3.97−3.52 (m, 7H), 3.52−3.45 (m, 1H), 3.46 (s, 1H), 3.20−3.11 (m, 1H), 2.98−2.86 (m, 1H), 2.77−2.63 (m, 3H), 2.34−2.10 (m, 2H), 1.80−1.72 (m, 1H), 1.70 (dd, J = 14.7, 7.4 Hz, 4H), 1.64 (s, 6H), 1.46 (q, J = 7.7 Hz, 2H), 1.31−1.20 (m, 2H), 1.18 (t, J = 6.6 Hz, 12H). ^{31}P{^{1}H} NMR (162 MHz, $CDCl_3$): δ 148.4, 148.2. Note: This compound is reactive and decomposed under ^{13}C NMR and MS conditions.

Synthesis of 6-*O*-{[6-*O*-[(2-*N*-Biotinyl-2-aminoethyloxy)-(2-cyanoethyloxy)-phosphono]-2,3,4-tri-*O*-(*p*-methoxybenzyl)-α-D-mannopyranosyl]-(1→2)-[3,4,6-tri-*O*-(*p*-methoxybenzyl)-α-D-mannopyranosyl]-(1→6)-[3,4-di-*O*-(*p*-methoxybenzyl)-2-*O*-(4-oxopentanoyl)-α-D-mannopyranosyl]-(1→4)-[2-azido-2-deoxy-3,6-di-*O*-(*p*-methoxybenzyl)-α-D-glucopyranosyl]}-1-*O*-[(2-cyanoethyloxy)-(2,3-di-*O*-stearoyl-*sn*-glycerol)-phosphono]-2,3,4,5-tetra-*O*-(*p*-methoxybenzyl)-*myo*-inositol (15). To a solution of **12** (7.90 mg, 2.34 μmol, 1.0 equiv) and 1*H*-tetrazole (0.45 M solution in acetonitrile, 0.2 mL, 93.6 μmol, 40 equiv) in anhydrous DCM (2.0 mL) under N_2 at rt was added a solution of freshly prepared phosphoramidite **14** (23.0 mg in 1.0 mL anhydrous DCM, 46.8 μmol, 20 equiv) dropwise with stirring. After stirring at rt under N_2 for 1 h, the reaction mixture was cooled to 0 °C and then iodine (11.9 mg, 46.8 μmol, 20 equiv) in a mixture of pyridine/water (9:1, v/v, 0.1 mL) was added. The solution was stirred for 10 min while being slowly warmed to rt and diluted with DCM. The mixture was poured into saturated aqueous $NaHCO_3$ and extracted with DCM (3 × 5 mL). The combined organic layers were dried over Na_2SO_4 and concentrated in vacuum. The product was purified using a size-exclusion LH-20 column eluted with MeOH/DCM (3:2) to give **15** (6.90 mg, 1.83 μmol, 76%) as pale-yellow syrup. ^{1}H NMR (600 MHz, $CDCl_3$, partial): δ 7.32−7.07 (m, 28 H), 6.88−6.78 (m, 28 H), 5.47 (s, 1H), 5.39 (s, 1H), 5.32 (s, 1H), 5.26 (s, 1H), 5.17−5.11 (m, 1H), 4.94 (m, 1H), 4.84 (m, 1H), 4.81−4.67 (m, 1H), 4.64 (s, 1H), 4.57 (m, 1H), 4.45−4.35 (m, 1H), 4.30 (s, 1H), 4.25 (s, 1H), 3.81 (s, 3 H), 3.78 (s, 3 H), 3.74−3.72 (s, multiple), 3.64 (s, 3 H), 3.62 (s, 3 H), 3.60 (s, 3H), 3.42 (s, 3 H), 2.81−2.53 (m, 1H), 2.35−2.26 (m, 1H), 2.12−2.07 (m, 3H), 1.59 (s, 6H), 1.32 (m, 2H), 1.31 (s, 6H), 1.27 (m, 56H), 0.90 (t, J = 7.0 Hz, 6H). ^{13}C{^{1}H} NMR (151 MHz, $CDCl_3$, derived from HSQC spectrum): δ 129.6−129.2 (multiple C), 113.8−113.7 (multiple C), 99.7 (Man-1), 99.2 (Man-1), 99.0 (Man-1), 97.7 ($GlcN_3$-1), 92.4, 81.3, 80.4 (2 C), 80.3, 79.5, 76.9, 76.5, 76.2, 75.3, 75.1, 75.0, 74.9 (2 C), 74.7 (3 C), 74.6 (2 C), 74.4, 73.8, 73.0 (2 C), 72.7 (2 C), 71.8 (4 C), 71.6 (2 C), 71.5, 70.6, 70.5, 69.7, 69.4 (2 C), 69.0, 68.7 (2 C), 68.1, 67.4, 67.2, 66.5, 66.4, 66.2, 66.1, 64.3, 63.1, 62.6, 62.4, 62.1, 61.7 (2 C), 61.5, 60.1, 59.9, 56.0, 55.2 (4 C), 55.1 (2 C), 50.8, 40.4 (2 C), 39.7, 38.0 (2 C), 35.6, 35.0, 34.0, 30.6, 29.8, 29.6, 28.0 (2 C), 25.8, 24.9, 22.7, 21.4, 21.1, 20.7, 19.7 (2 C), 19.2, 14.1 (2 C), 13.8, 10.9, 8.5, 8.4. ^{31}P NMR (243 MHz, $CDCl_3$): δ −1.2, −2.3, −2.4, −3.1. HR ESI-TOF-MS m/z: Calcd for $C_{204}H_{278}N_{10}O_{53}P_2S$ $[M + 2NH_4]^{2+}$, 1904.9276; found, 1904.9280.

Synthesis of 6-*O*-{[6-*O*-[(*N*-Biotinyl-2-aminoethyloxy)-phosphono]-α-D-mannopyranosyl]-(1→2)-(α-D-mannopyranosyl)-(1→6)-(α-D-mannopyranosyl)-(1→4)-(2-amino-2-deoxy-α-D-glucopyranosyl)}-1-*O*-[(2,3-di-*O*-stearoyl-*sn*-glycerol)-phosphono]-*myo*-inositol (1). Hydrazine acetate (2.00 mg) was added to a solution of **15** (6.80 mg, 1.80 μmol) in THF (4.0 mL), and the resulting mixture was stirred at rt for 2 h. ESI MS data showed the complete deprotection of the levulinic group (m/z calcd for $C_{199}H_{264}N_8O_{51}P_2SNa$ $[M + Na]^+$ 3398.7; found, 3398.6). Then brine was added, and the mixture was extracted with EtOAc (3 × 5 mL). The combined organic phase was dried over Na_2SO_4, filtered, and concentrated under vacuum. The crude product was then dissolved in pyridine/H_2O (4:1, v/v, 1 mL), and then 1,3-propanedithiol (0.1 mL) and DIPEA (0.2 mL) were added. The reaction mixture was stirred at rt for 36 h, and ESI MS data showed the complete reduction of the azide and deprotection of the cyanoethyl group (m/z calcd for $C_{199}H_{264}N_8O_{51}P_2S$ $[M - 2H]^{2-}$, 1770.8; found, 1770.9). The mixture was concentrated under vacuum to dryness, and the residue was subjected to Sephadex LH-20 size exclusion column chromatography (eluent: DCM/MeOH = 1:1) to provide the intermediate as colorless syrup. Next, the product was dissolved in DCM (1.4 mL), which was followed by addition of TFA (150 μL) to form a solution of ∼10% TFA in DCM (v/v). After stirring for 20 min, the reaction mixture was diluted with toluene and condensed under vacuum. The mixture was coevaporated with toluene five times. Finally, the crude product was purified by size exclusion column chromatography (eluent: $CHCl_3$/MeOH/H_2O = 10:9:1) using Sephadex LH-20 to afford **1** (2.70 mg, 1.45 μmol, 80%) as a white solid. ^{1}H NMR (600 MHz, $CDCl_3$/MeOD/D_2O = 9:10:1, partial): δ 5.24 (m, 1 H, Gly-2), 5.17 (s, 1 H, $GlcNH_2$-1), 5.15 (s, 1 H, Man-1), 5.13 (s, 2 H, $-CH_2-$), 4.95 (s, 2 H, including two Man-1) 2.36−2.17 (m, 4 H, $-CH_2-$) 1.58 (m, 8 H), 1.33−1.22 (m, 56 H), 0.88 (t, J = 6.9 Hz, 6 H). ^{13}C{^{1}H} NMR (151 MHz, $CDCl_3$/MeOD/D_2O = 9:10:1, derived from HSQC spectrum): δ 102.5 (2 Man-1), 101.4 (Man-1), 98.1 ($GlcNH_2$-1), 79.4, 77.3, 77.0, 76.3, 72.7, 72.2, 71.6, 70.9, 70.6, 70.5, 70.3(2 C), 70.2, 66.9, 66.8, 65.0, 64.0, 63.6, 62.8 (2 C), 62.7, 62.0, 61.4 (2 C), 60.2 (2 C), 57.1, 55.7, 55.5, 55.2, 55.1, 54.2, 41.6, 40.2 (2 C), 40.0, 38.0, 36.2, 36.1, 35.5, 34.2, 34.0, 33.6, 30.9, 29.6, 28.2, 27.9, 26.7, 25.7 (2 C), 24.9, 24.8, 22.6 (multiple C), 22.1, 19.5, 19.4, 13.8. ^{31}P{^{1}H} NMR (243 MHz, $CDCl_3$/MeOD/D_2O = 9:10:1): δ 0.7, −0.2. HR ESI-TOF-MS (negative mode) m/z: calcd for $C_{81}H_{146}N_4O_{37}P_2S$ $[M - 2H]^{2-}$, 930.4436; found, 930.4439.

Liposome Preparation. To a solution of biotinylated GPI **1** (133 μL, 0.1 μmol) in chloroform was added POPC (7.60 mg, 10.0 μmol) to generate a homogeneous solution. The solvent was removed via rotary evaporation under reduced pressure, and the resultant lipid mixture was kept under high vacuum overnight to remove any residual solvent. The negative control group contained only POPC. To the dry lipid sample was added HEPES buffer (5 mM, pH 7.5, 1 mL) at rt, and the mixture was sonicated at rt for 15 s and then vigorously vortexed for 2 min. The suspension was frozen in liquid nitrogen and thawed at rt, and the freeze−thaw cycle was repeated five times. The suspension was extruded 31 times through a polycarbonate filter with pore size of 100 nm at rt using an Avanti Mini-Extruder System (Avanti Polar Lipids, Inc.) to provide a suspension of the desired unilamellar liposomes. The size of the liposomes was characterized by dynamic light scattering (DLS) to be 100 nm with a polydispersity (PDI) of 0.16, using a Zetasizer Nano Light Scattering System (Malvern Panalytical, Inc.).

Investigation of Liposomes by ELISA. Streptavidin (20.0 μg/mL) in coating buffer (0.1 M bicarbonate, pH 9.6) was added to each well of an ELISA plate (100 μL/well), and the plate was incubated at 4 °C overnight and 37 °C for 1 h, which was followed by washing using phosphate-buffered saline with Tween 20 (PBST) buffer three times. Thereafter, the blocking buffer of PBST containing 1% bovine serum albumin (BSA) (200 μL/well) was added to each well, and the plate was incubated at rt for 1 h and washed with PBST (3×). Liposome suspensions prepared above were added to the plate (20 μL/well), which was incubated at 37 °C for 2 h and washed with PBST (3×). Next, streptavidin-AP (1:1000 dilution in PBS, 100 μL/well) was added, followed by incubation at rt for 1 h and washing with PBST (3×), and then addition of PNPP in PBS (1.67 mg/mL, 100 μL/well). The plate was kept at rt for 30 min before the light absorbance was measured at 405 nm wavelength using a plate reader (Cytation 1, Bio-Tek Instruments Inc.). For fluorescence analysis,

https://doi.org/10.1021/acs.joc.3c02560
J. Org. Chem. 2024, 89, 1345−1352

after the addition of liposomes to the plate, streptavidin-A488 (1:500 dilution in PBS, 100 μL/well) was added, and the plate was incubated at rt for 1 h and washed with PBST (3×). Finally, PBS (100 μL/well) was added to the plate, which was followed by fluorescence intensity measurement using a plate reader. Each experiment was repeated three times.

Investigation of Liposomes in Solution. To the liposome suspension obtained above (300 μL) was added streptavidin-A488 (1.0 μL, 1.00 mg/mL in PBS). After the suspension was incubated at rt for 1 h, it was transferred into a 100 kDa MWCO centrifugal filter unit and then centrifugated at 3000 rpm for 10 min. Thereafter, PBS (1.0 mL) was added to the unit, which was followed by centrifugation again. This process to remove non-membrane-bound streptavidin-A488 using 100 kDa cut filter and centrifugation, which also concentrated the liposome−GPI−biotin−streptavidin−A488 conjugate, was repeated at least five times, until the filtrate harvested after washing did not show significant fluorescence. Finally, the fluorescence intensities of streptavidin−A488-treateed liposomes were measured using a microplate reader. This experiment was repeated three times.

Statistical Analysis. All data were analyzed by independent *t*-test (to compare data between two groups), using GraphPad software. $P < 0.05$ was considered statistically significant.

■ ASSOCIATED CONTENT

Data Availability Statement

The data underlying this study are available in the published article and its Supporting Information.

Supporting Information

The Supporting Information is available free of charge at https://pubs.acs.org/doi/10.1021/acs.joc.3c02560.

Additional experimental procedures, results of biological evaluations, and NMR and MS spectra of all new compounds and other key intermediates (PDF)

■ AUTHOR INFORMATION

Corresponding Author

Zhongwu Guo − *Department of Chemistry, University of Florida, Gainesville, Florida 32611, United States; UF Health Cancer Centre, University of Florida, Gainesville, Florida 32611, United States;* orcid.org/0000-0001-5302-6456; Email: zguo@chem.ufl.edu

Authors

Xin Yan − *Department of Chemistry, University of Florida, Gainesville, Florida 32611, United States;* orcid.org/0000-0003-1846-3241

Jiatong Guo − *Department of Chemistry, University of Florida, Gainesville, Florida 32611, United States*

Sayan Kundu − *Department of Chemistry, University of Florida, Gainesville, Florida 32611, United States*

Complete contact information is available at: https://pubs.acs.org/10.1021/acs.joc.3c02560

Author Contributions

The manuscript was written through contributions of all authors. All authors approved the final version of the manuscript.

Author Contributions

[§]These authors contributed equally to the present work.

Notes

The authors declare no competing financial interest.

■ ACKNOWLEDGMENTS

This work is supported by NIH/NIGMS (1R35 GM131686). The MS instrument was funded by NIH (S10 OD021758). Z.G. is also grateful to Steven and Rebecca Scott for endowing our research.

■ REFERENCES

(1) Ferguson, M. A. J. The structure, biosynthesis and functions of glycosylphosphatidylinositol anchors, and the contributions of trypanosome research. *J. Cell Sci.* **1999**, *112*, 2799−2809.

(2) Thomas, J. R.; Dwek, R. A.; Rademacher, T. W. Structure, biosynthesis, and function of glycosylphosphatidylinositols. *Biochemistry* **1990**, *29*, 5413−5422.

(3) Paulick, M. G.; Bertozzi, C. R. The glycosylphosphatidylinositol anchor: A complex membrane-anchoring structure for proteins. *Biochemistry* **2008**, *47*, 6991−7000.

(4) Kinoshita, T. Biosynthesis and biology of mammalian GPI-anchored proteins. *Open Biol.* **2020**, *10*, No. e190290.

(5) Borges, A. R.; Link, F.; Engstler, M.; Jones, N. G. The glycosylphosphatidylinositol anchor: A linchpin for cell surface versatility of trypanosomatids. *Front. Cell Dev. Biol.* **2021**, *9*, No. e720536.

(6) Eckert, V.; Gerold, P.; Schwarz, R. T. GPI-anchors: Structure and functions. In *Glycosciences*; Gabius, H.-J.; Gabius, S., Eds.; Chapman & Hall: Weinheim, Germany, 1997; pp 223−243.

(7) Hwa, K. Glycosyl phosphatidylinositol-linked glycoconjugates: Structure, biosynthesis and function. *Adv. Exp. Med. Biol.* **2001**, *491*, 207−214.

(8) Pittet, M.; Conzelmann, A. Biosynthesis and function of GPI proteins in the yeast Saccharomyces cerevisiae. *Biochim. Biophys. Acta* **2007**, *1771*, 405−420.

(9) Zhou, K. Glycosylphosphatidylinositol-anchored proteins in *Arabidopsis* and one of their common roles in signaling transduction. *Front. Plant Sci.* **2019**, *10*, 1022.

(10) Robinson, P. J. Signal transduction by GPI-anchored membrane proteins. *Cell Biol. Int. Rep.* **1991**, *15*, 761−767.

(11) Trotter, J.; Klein, C.; Kramer, E. GPI-anchored proteins and glycosphingolipid-rich rafts: Platforms for adhesion and signaling. *Neuroscientist* **2000**, *6*, 271−284.

(12) Tiveron, M. C.; Nosten-Bertrand, M.; Jani, H.; Garnett, D.; Hirst, E. M.; Grosveld, F.; Morris, R. J. The mode of anchorage to the cell surface determines both the function and the membrane location of Thy-1 glycoprotein. *J. Cell Sci.* **1994**, *107*, 1783−1796.

(13) Bate, C.; Williams, A. Monoacylated cellular prion protein modifies cell membranes, inhibits cell signaling, and reduces prion formation. *J. Biol. Chem.* **2011**, *286*, 8752−8758.

(14) Puig, B.; Altmeppen, H. C.; Linsenmeier, L.; Chakroun, K.; Wegwitz, F.; Piontek, U. K.; Tatzelt, J.; Bate, C.; Magnus, T.; Glatzel, M. GPI-anchor signal sequence influences PrPC sorting, shedding and signalling, and impacts on different pathomechanistic aspects of prion disease in mice. *PLoS Pathog.* **2019**, *15*, No. e1007520.

(15) Bate, C.; Tayebi, M.; Williams, A. The glycosylphosphatidylinositol anchor is a major determinant of prion binding and replication. *Biochem. J.* **2010**, *428*, 95−101.

(16) Bate, C.; Nolan, W.; Williams, A. Does the tail wag the dog? How the structure of a glycosylphosphatidylinositol anchor affects prion formation. *Prion* **2016**, *10*, 127−130.

(17) Taguchi, R.; Hamakawa, N.; Harada-Nishida, M.; Fukui, T.; Nojima, K.; Ikezawa, H. Microheterogeneity in glycosylphosphatidylinositol anchor structures of bovine liver 5′-nucleotidase. *Biochemistry* **1994**, *33*, 1017−1022.

(18) Paulick, M. G.; Wise, A. R.; Forstner, M. B.; Groves, J. T.; Bertozzi, C. R. Synthetic analogues of glycosylphosphatidylinositol-anchored proteins and their behavior in supported lipid bilayers. *J. Am. Chem. Soc.* **2007**, *129*, 11543−11550.

(19) Becker, C. F. W.; Liu, X.; Olschewski, D.; Castelli, R.; Seidel, R.; Seeberger, P. H. Semisynthesis of a glycosylphosphatidylinositol-anchored prion protein. *Angew. Chem., Int. Ed.* **2008**, *47*, 8215−8219.

(20) Roller, R. F.; Malik, A.; Carillo, M. A.; Garg, M.; Rella, A.; Raulf, M.-K.; Lepenies, B.; Seeberger, P. H.; Varón Silva, D. Semisynthesis of functional glycosylphosphatidylinositol-anchored proteins. *Angew. Chem., Int. Ed.* **2020**, *59*, 12035−12040.
(21) Guo, X.; Wang, Q.; Swarts, B. M.; Guo, Z. Sortase-catalyzed peptide-glycosylphosphatidylinositol analog ligation. *J. Am. Chem. Soc.* **2009**, *131*, 9878−9879.
(22) Wu, Z.; Guo, X.; Wang, Q.; Swarts, B. M.; Guo, Z. Sortase A-catalyzed transpeptidation of glycosylphosphatidylinositol derivatives for chemoenzymatic synthesis of GPI-anchored proteins. *J. Am. Chem. Soc.* **2010**, *132*, 1567−1571.
(23) Wu, Z.; Guo, X.; Gao, J.; Guo, Z. Sortase A-mediated chemoenzymatic synthesis of complex glycosylphosphatidylinositol-anchored protein. *Chem. Commun.* **2013**, *49*, 11689−11691.
(24) Xue, J.; Shao, N.; Guo, Z. First total synthesis of a GPI-anchored peptide. *J. Org. Chem.* **2003**, *68*, 4020−4029.
(25) Shao, N.; Xue, J.; Guo, Z. Chemical synthesis of a skeleton structure of sperm CD52 - A GPI-anchored glycopeptide. *Angew. Chem., Int. Ed.* **2004**, *43*, 1569−1573.
(26) Zhu, S.; Guo, Z. Chemical synthesis of GPI glycan-peptide conjugates by traceless Staudinger ligation. *Org. Lett.* **2017**, *19*, 3063−3066.
(27) Dhar, T.; Mootz, H. D. Modification of transmembrane and GPI-anchored proteins on living cells by efficient protein trans-splicing using the Npu DnaE intein. *Chem. Commun.* **2011**, *47*, 3063−3065.
(28) Elia, G. Biotinylation reagents for the study of cell surface proteins. *Proteomics* **2008**, *8*, 4012−4024.
(29) Hermanson, G. T. (Strept)avidin-biotin systems. In *Bioconjugate Techniques*, 3rd ed.; Hermanson, G. T., Ed.; Elsevier, Rockford, IL, 2013; pp 465−505.
(30) Green, N. M. Avidin. 3. The nature of the biotin-binding site. *Biochem. J.* **1963**, *89*, 599−609.
(31) Livnah, O.; Bayer, E. A.; Wilchek, M.; Sussman, J. L. Three-dimensional structures of avidin and the avidin-biotin complex. *Proc. Natl. Acad. Sci. U.S.A.* **1993**, *90*, 5076−5080.
(32) Yan, X.; Guo, Z. Diversity-oriented synthesis of glycosylphosphatidylinositol probes based on an orthogonally protected pentasaccharide. *Org. Lett.* **2023**, *25*, 2088−2092.
(33) Swarts, B. M.; Guo, Z. Synthesis of a glycosylphosphatidylinositol (GPI) anchor carrying unsaturated lipid chains. *J. Am. Chem. Soc.* **2010**, *132*, 6648−6650.
(34) Swarts, B. M.; Guo, Z. Chemical synthesis and functionalization of clickable glycosylphosphatidylinositol anchors. *Chem. Sci.* **2011**, *2*, 2342−2352.
(35) van Boom, J. H.; Burgers, P. M. J. Use of levulinic acid in the protection of oligonucleotides via the modified phosphotriester method: Synthesis of decaribonucleotide u-a-u-a-u-a-u-a-u-a. *Tetrahedron Lett.* **1976**, *17*, 4875−4878.
(36) Schmidt, R. R.; Michel, J. Simple syntheses of α- and β-O-glycosyl imidates: Preparation of glycosides and disaccharides. *Angew. Chem., Int. Ed.* **1980**, *19*, 731−733.
(37) Duynstee, H. I.; de Koning, M. C.; Ovaa, H.; van der Marel, G. A.; van Boom, J. H. Synthesis of verbascoside: A dihydroxyphenylethyl glycoside with diverse bioactivity. *Eur. J. Org. Chem.* **1999**, *1999*, 2623−2632.
(38) Kayushin, A.; Demekhina, A.; Korosteleva, M.; Miroshnikov, A.; Azhayev, A. Synthesis of biotin-containing phosphoramidite linker with polyether spacer arm. *Nucleosides Nucleotides Nucleic Acids* **2011**, *30*, 490−502.
(39) Jones, A. S.; McGuigan, C.; Walker, R. T. Synthesis of some nucleoside cyclic phosphoramidates and related compounds via phosphoramidites. *J. Chem. Soc., Perkin Trans. 1* **1985**, 199−202.
(40) Dorman, M. A.; Noble, S. A.; McBride, L. J.; Caruthers, M. H. Synthesis of oligodeoxynucleotides and oligodeoxynucleotide analogs using phosphoramidite intermediates. *Tetrahedron* **1984**, *40*, 95−102.
(41) Upadhya, K.; Khattak, I. K.; Mullah, B. Oxidation of biotin during oligonucleotide synthesis. *Nucleosides Nucleotides Nucleic Acids* **2005**, *24*, 919−922.
(42) Rebhan, M. A.; Brunschweiger, A.; Hall, J. Measurement by SPR of very low dissociation rates: Oxidation-mediated loss of biotin-streptavidin affinity. *ChemBioChem.* **2013**, *14*, 2091−2094.
(43) Mock, D. M.; Lankford, G. L.; Mock, N. I. Biotin accounts for only half of the total avidin-binding substances in human serum. *J. Nutr.* **1995**, *125*, 941−946.
(44) Mock, D. M.; Mock, N. I. Serum concentrations of bisnorbiotin and biotin sulfoxide increase during both acute and chronic biotin supplementation. *J. Lab. Clin. Med.* **1997**, *129*, 384−388.
(45) Zhang, H. Thin-film hydration followed by extrusion method for liposome preparation. *Methods Mol. Biol.* **2017**, *1522*, 17−22.

https://doi.org/10.1021/acs.joc.3c02560
J. Org. Chem. 2024, 89, 1345−1352